Condition Indicators for Gears

Dr. Renata Klein

R.K. Diagnostics, Gilon, POB 101, D.N. Misgav, 20103, Israel
renata.klein@rkdiagnostics.co.il

ABSTRACT

Diagnostics of faults in gears requires development of reliable condition indicators. A large number of condition indicators, which are based on statistical moments of the synchronous average and its derivatives (difference and residual signals) were previously suggested. This study evaluates the efficiency of different gear condition indicators that are based on statistical moments and compares them with two new types of condition indicators that are suggested. The two new types of condition indicators are based on the order spectrum and the spectral kurtosis of the synchronous average.

The study was conducted on the labeled data of PHM'09 challenge. This data included recordings of vibrations in helical and spur gearboxes with seeded faults.

1. INTRODUCTION

Vibration based diagnostics of gears based on statistical moments of the synchronous average was investigated before (Dempsey & Zakrajsek 2001, Lebold, McClintic, Campbell, Byington & Maynar, 2000, Mosher, Pryor & Huff, 2002, Zacksenhous, Braun, Feldman & Sidahmed, 2000). Many different condition indicators have been proposed for different types of gear malfunctions. An automatic diagnostic process for gears requires selecting a set of the relevant condition indicators and aggregating them into health indicators.

The selection of condition indicators is based on their ability to detect the faults with minimum false alarms, i.e. their ability to differentiate between faulty and healthy states with the maximum contrast, and if possible to indicate the type of fault. Hence, the evaluation of condition indicators should be conducted with healthy recordings as well as recordings of different seeded faults.

The evaluation of the condition indicators was performed using the labeled data from PHM'09 challenge. It contains records of both spur and helical gears, split between two load levels, healthy or with three types of faults: broken tooth, chipped tooth, and eccentricity. The presence of different faults allows selection of condition indicators covering more than one type of fault.

The data that was used is briefly described in chapter 2. Chapter 3 presents the signal processing procedure, and chapter 4 describes the condition indicators that were evaluated. Chapter 5 presents and discusses the results.

2. PHM' 09 CHALLENGE LABELED DATA

The PHM'09 data set included 280 recordings of 4 seconds each, measured on the gearbox described in Figure 1 (from Klein, Rudyk, Masad & Issacharoff, 2011b), using two vibration sensors (Sin and Sout) and a tachometer. All the bearings were similar. Some of the signals were recorded when the gearbox was in 'spur' configuration, and others when it was in 'helical' configuration. Data were collected at 30, 35, 40, 45 and 50 Hz shaft speeds, under high and low loading (HL and LL) (Klein, Rudyk, Masad & Issacharoff, 2011b) .

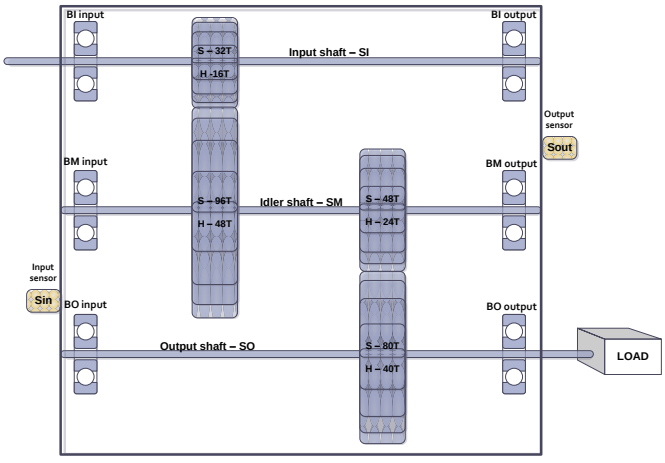

Figure 1. Challenge apparatus: spur (S) and helical (H) configurations

In the challenge apparatus, in spur and helical configurations, the idler shaft (SM) and the output shaft

(SO) rotated at 1/3 and 1/5 of the rotating speed of the input shaft (SI) correspondingly. The gear ratios generated overlapping characteristic frequencies that made the separation between the manifestations of different gearwheels especially challenging.

Table 1 summarizes the recordings of the PHM'09 data set and the damages that were present on the gears.

Case	Gears				Bearings			Shaft	
	32T	96T	48T	80T	bSI	bSM	bSO	Input	Output
Spur 1	Good		Good						
Spur 2	Chipped		Eccentric	Good		Good			
Spur 3			Eccentric					Good	
Spur 4	Good	Good	Eccentric	Broken	Ball	Good	Good		
Spur 5	Chipped		Eccentric	Broken	Inner	Ball	Outer		
Spur 6	Good		Good	Broken	Inner	Ball	Outer	Imbalance	Good
Spur 7					Inner	Good	Good	Good	Key
Spur 8	Good		Good		Good	Ball	Outer	Imbalance	Good
	16T	48T	24T	40T					
Helical 1			Good						
Helical 2			Chipped			Good		Good	
Helical 3			Broken		Comb	Inner		Bent	
Helical 4	Good		Good	Good	Comb	Ball	Good	Imbalance	Good
Helical 5			Broken		Good	Inner		Good	
Helical 6			Good			Good		Bent Shaft	Good

Table 1. PHM'09 challenge dataset faults

3. GEAR SIGNAL ANALYSIS

The most widely used signatures in gear analysis are computed in the order, the quefrency of orders and the cycle domains (Klein et al. 2011b, Lebold et al. 2000, Zacksenhouse et al. 2000). The time history is mapped into the cycle domain after synchronization (resampling) according to the shaft rotating speed.

The cepstrum of the orders representation was generated as follows:

$$C_v := \Re\{\mathcal{F}^{-1}[ln(\mathcal{F}[v(t)])]\} \quad (1)$$

where: C_v is the real cepstrum of $v(t)$.

The cepstrum reflects the repetition rate of the sidebands (due to frequency modulation) and their average level in several peaks in the quefrency of orders domain (Zacksenhouse et al. 2000, Antoni & Randall 2002).

The separation of the vibrations that belong to a certain gearwheel is achieved by calculating the synchronous average according to the respective shaft speed (Antoni & Randall 2002, Mosher et al. 2002, Zacksenhouse et al. 2000). Averaging is applied to enhance deterministic effects synchronized with the rotation of the relevant shaft. The synchronous average signal reveals the vibration induced by the meshing of each tooth on the relevant gearwheel.

The synchronous average removes the asynchronous components by averaging the resampled signal in each rotation cycle. All the signal elements that are not in phase with the rotation speed are eliminated, leaving the periodic elements present in one cycle, i.e. the elements corresponding to the harmonics of the shaft rotating speed (Klein, Rudyk, Masad & Issacharoff, 2011a).

Synchronous average with frequency f is designed to remove elements in v which are not periodic with the period $N=1/f$.

$$y_n := \frac{1}{M}\sum_{m=0}^{M-1} v_{n+mN} \quad n = 1, \cdots, N \quad (2)$$

Note that y is a vector in $\mathbb{R}^N$ representing a single cycle.

The synchronous average ability to filter out the asynchronous elements depends on the number of cycles averaged (in this case M). Therefore, it is preferable to average as many cycles as possible. In the case of the PHM recordings, the number of cycles averaged differed pending on the shaft rotating speed. For the input shaft, the number of cycles averaged was 120-200 depending on the rotating speed (RPS of 30-50Hz respectively). The number of cycles averaged for the idler shaft was in the range 40-66, and for the output shaft in the range of 24-40.

Detection of abnormal meshing of an individual tooth is achieved by further processing of the averaged signal in three types of signals: regular, residual, and difference (Klein et al. 2011b, Mosher et al. 2002, Zacksenhouse et al. 2000). The regular signals are obtained by passing the synchronous-averaged signal through a multi-band-pass filter, with pass-bands centered at the meshing frequency and its harmonics (1÷5). It is essentially the cycle-domain average of the vibrations induced by a single tooth. The residual signals are obtained by removing the meshing frequency harmonics. The difference signals are obtained by removing the meshing frequencies and the adjacent sidebands (in that study, two sidebands have been removed), i.e. the frequency and amplitude modulations were separated.

The envelopes of the regular, difference and residual parts of all the harmonics describe the characteristics of the amplitude modulation.

In order to better separate the excitations from the gearwheels on different shafts, the synchronous averages according to the idler and output shafts were calculated using a dephased signal (Klein et al. 2011a) by the input shaft (see Figure 16). As a result, the integer multiples of the input shaft that coincide with every third multiple of the idler shaft and every fifth multiple of the output shaft were removed, leaving only partial information related to the respective gearwheels but isolating the excitations from the gearwheel on the input shaft.

The spectral kurtosis denoted SK of the synchronous average according to every shaft was calculated according to equation 3 (Antoni, 2006).

$$SK = K_y(f) := \frac{S_{4y}(f)}{S_{2y}^2(f)} - 2, \quad f \neq 0 \quad (3)$$

where: $S_{2ny}(f) = \langle S_{2ny}(t,f)\rangle_t = E\left\{\left|S_y(t,f)\right|^{2n}\right\}/df$ is the average *2n* power of the spectrum, *f* denotes frequency, and *t* denotes time. For *n*=1, we obtain the power spectral density.

The spectral kurtosis is a statistical tool, which can indicate the presence of transients and their location in the frequency domain (in our case order domain). The SK provides a robust way of detecting incipient faults even in the presence of a strong masking noise (Antoni & Randall 2004).

In order to diagnose each gearwheel separately, the spectral kurtosis was not calculated on the raw or resampled signals as it is usually done. Instead, it was calculated on the synchronous average according to each shaft (see Figure 16). This approach was especially needed for the PHM'09 challenge data because in most of the recordings with faulty gears, there were other faulty components that could affect the spectral kurtosis (e.g. bearings, see Table 1). The spectral kurtosis was calculated on windows of ¼ cycles with 50% overlapping, generating a spectrum with resolution of four orders. The averaging of windows corresponding to ¼ cycle was a compromise to overcome the problem of short recordings.

When longer recordings are available, (e.g. more than 200 cycles for all the operating conditions), it is recommended to calculate several synchronous averages on running windows of more than 20 cycles, and then calculate the spectral kurtosis on windows corresponding to one cycle.

4. FEATURE EXTRACTION

The proposed process for feature extraction is in essence a comparison of the analyzed signatures to the "baseline" population (a model of normality), i.e. determination of the Mahalanobis distance between the analyzed signature and the baseline (Klein, Rudyk & Masad, 2011c).

The usage of distance signatures generates features (condition indicators) in terms of distance from the "normal" in σ units, allowing application of generic decision and fusion algorithms for each type of component. The weakness of the process is in the hidden assumption of Gaussian distribution of the values in the signatures when using Mahalanobis distances. As will be shown below, some methods will be used to overcome this weakness.

4.1. Baselines

Baselines are signatures derived from healthy recordings, in the considered domains. Each set of such signatures represents the statistics of healthy signatures in a certain predefined operating mode. The baselines are usually the spectra (orders) or statistical moments, representing average, variance, median and estimator of the standard deviation (normalized IQR inter-quartile range $\tilde{\sigma} = IQR \cdot 0.7413$) of the signatures that compose it.

For the gear diagnostics of the PHM'09 data, the baseline signatures were generated using an expanded set of records that included all the records of healthy machines plus all the records in which the gears were healthy but not necessarily the bearings or the shafts. This was done to enhance the quality of the baselines by including as many records as possible. The justification for this approach emerges from the facts that it is possible to screen out the excitations from bearing faults by using the synchronous average, and it is possible to screen out the excitations from shaft faults by using special filters.

4.2. Gear Features

Generally, gear meshing components, some low-order amplitude modulation components and/or phase modulation components dominate the synchronous average. These modulation effects are generated by transmission errors related to geometric and assembly errors of the gear pairs. When a localized gear fault is present, a short period impulse will appear in each complete revolution. This produces additional amplitude and phase modulation effects. Due to its short period, the impulse produces high order low-amplitude sidebands surrounding the meshing harmonics in the spectrum. The removal of the regular gear meshing harmonics (residual part) sometimes with their low-order sidebands (difference part) from the synchronous average emphasizes the portion predominantly caused by gear fault and geometrical and assembly errors. Statistical measures of the difference and residual parts are used to quantify the fault-induced shocks, e.g. condition indicators like FM0, FM2, FM4, FM6, FM8, NA4, NB4, etc. (Lebold et al. 2000, Mosher et al. 2002, Dempsey & Zakrajsek, 2001).

The short impulse generated in each revolution is expected to be revealed in the spectral kurtosis of the synchronous average at the orders corresponding to the frequency contents of the impulse. It should be mentioned that high levels are not expected at the gearmesh or sidebands orders and probably will be only manifested at high orders where the spectrum levels are relatively low (Antoni, 2006).

4.3. Gear Feature Extraction for PHM'09 data

The features (condition indicators) of gears were extracted for both the spur and helical configurations based on the distance signatures.

The features extracted for each gear wheel in the cycles domain included: the even statistical moments (RMS and kurtosis) of the regular, residual and difference parts, the even moments of the envelope of the regular, residual and difference.

The distances of the cepstrum representing the orders-quefrency of the respective shafts where extracted as well.

The spectral kurtosis distances from the baselines according to each shaft were calculated. The purpose of this was to investigate their ability to detect gear faults. The condition indicator extracted from the spectral kurtosis distance signatures was the sum of values exceeding 3σ .

The distance signatures of the order representations of the synchronous average according to each shaft were generated. The peak values at each harmonic of the shaft rotating speed (representing gearmesh orders and sidebands) were stored as features characterizing the gears. These peak values distances have been separated into three categories and grouped by their corresponding harmonics (Figure 2):

- AM – the sidebands representing amplitude modulation, i.e. the two low-order sidebands around the gear meshing orders
- FM – the sidebands representing frequency modulation, i.e. high-order sidebands around gear meshing orders
- GM – the gear meshing orders

The average distances D_h of the FM and AM peaks per every harmonic h were defined:

$$D_h = \frac{\sum_{i=1}^{N}(Y_i - \mu_i)}{\sqrt{\sum_{i=1}^{N}\sigma_i^2}} \quad (4)$$

where: i is the index of the peak, N is the pattern size (total number of sidebands considered for the FM or AM category in harmonic h), Y_i – the peak levels, μ_i – the corresponding mean level in the baseline, and σ_i – the corresponding standard deviation of the baseline. Because the average was used, it was possible to overcome the potential problem of non-Gaussian distributions (according to the Central Limit theorem, sums of variables tends to have a Gaussian distribution).

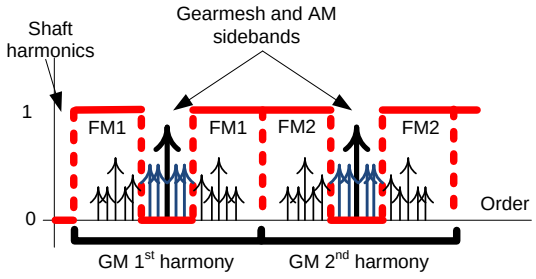

Figure 2. Illustration of the categories of peaks extracted in the orders of the synchronous average: FM1, FM2 denotes the group of sidebands of frequency modulation of the corresponding harmonic, the AM sidebands are drowed with blue arrows and the GM peaks with heavy black arrows.

5. CONDITION INDICATORS EVALUATION

It should be pointed out that in the PHM apparatus, it was especially difficult to identify the exact location of the faults, because the number of teeth on the gearwheels were exact multiples of each other. Since the gear mesh orders were exact multiples, demodulation was impractical. All the signatures and features were affected by mechanisms associated with the cross-gear interference (vibrations induced by one gear are modulated by vibrations of another gear). For instance, a fault in the input pinion gear may cause a modulation of the tooth meshing frequency with the tooth meshing of the large gearwheel, resulting in an erroneous identification of the fault location.

The features that have been evaluated and compared are averaged AM and FM modulations, the even statistical moments of the regular synchronous average, residual and difference signals, and the spectral kurtosis exceptions from baseline.

The kurtosis of all the signals did not reveal any type of fault in the PHM'09 dataset.

The RMS of the regular, difference, residual signals and their envelopes revealed similar detection abilities. Because of that, only the results of the RMS of the difference signal are shown and discussed.

Except for the spectral kurtosis, the evaluation was performed on features corresponding to the first three harmonics of the gearmesh only (Figure 2). We found out that the features of the higher harmonics did not contain additional meaningful fault detection information.

The following graphs present results for all the records in a specific configuration (spur or helical). The colors in the graphs are proportional to the distances from the baseline, usually in the range 6-30σ (a color bar is displayed on each figure). The vertical axis represents recordings corresponding to different rotating speed and low or high loads, denoted by the nominal rotating speed and HL for high load or LL for low load. The horizontal axis represents the different records for the specific configuration.

5.1. Helical configuration

In the helical configuration, the gearwheel with 48 teeth (GM2) on the idler shaft (SM) had a chipped tooth in run 2, and a broken tooth on runs 3 and 5. GM2 features corresponding to the first harmonic are displayed in Figure 3, Figure 4, and Figure 5. The results for higher harmonics were similar and therefore not displayed.

As can be observed in Figure 3 and in Figure 4, the RMS and the average distance of the AM and FM peaks were not able to detect the faulty gearwheel. In Figure 3, results of the FM and AM averages of the input sensor are presented separately showing that both were not able to reveal the faulty gearwheel.

Only the spectral kurtosis seems to reveal the faulty gearwheel reliably (the color range in Figure 5 is

approximately 6-100σ for both sensors). The levels of the spectral kurtosis sum are higher for the high load records.

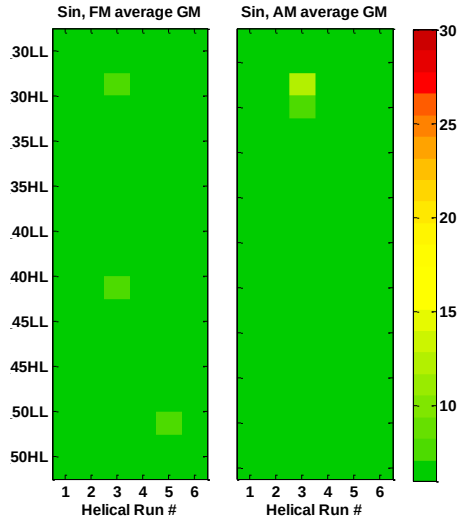

Figure 3. Average FM and AM sidebands, gearwheel GM2, harmonic 1, sensor Sin, helical runs: left average distance of FM sidebands, right average distance of AM sidebands.

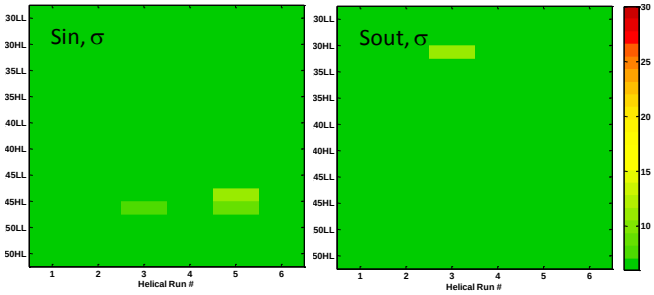

Figure 4. RMS of difference signal, harmonic 1, gearwheel, GM2, helical runs: left sensor Sin, right sensor Sout.

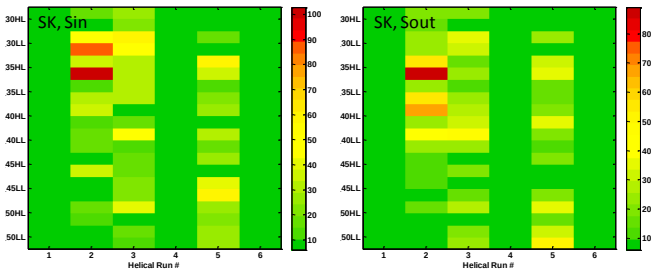

Figure 5. Sum of SK distances, gearwheel GM2, helical runs: left sensor Sin, right sensor Sout.

In general, the gear faults in the helical configuration displayed lower levels in all types of features and therefore were more difficult to detect. Usually, faults in helical gears can be better detected if the accelerometers are positioned in the axial direction. Unfortunately, both sensors in the PHM'09 dataset were radial.

5.2. Spur configuration

In spur configuration, runs 2-6 contained gear faults, mostly combinations of two or more faulty gearwheels.

5.2.1. Input gear results

In the spur configuration, one tooth of the input gearwheel (GI) was chipped in runs 2 and 5. The analysis results are presented in Figure 6, Figure 7, and Figure 8.

As can be observed in Figure 6, the average distance of the AM and FM sidebands allows good detection of the faulty runs (2 and 5) mainly in runs with high loads. Run 2 displayed lower distance values (probably because in run 5 there were 3 faulty gears that interfered with each other while in run 2 there were only two faulty gears). Run 2 was better detected in the sensor at the output (Sout).

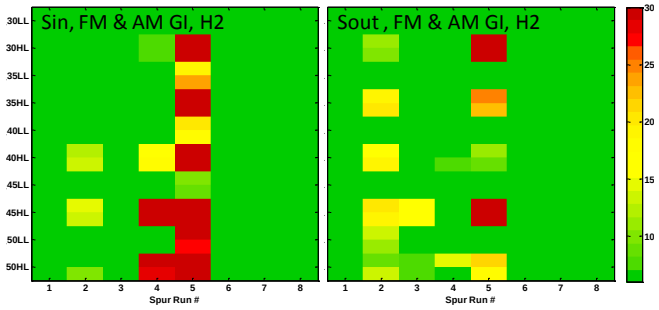

Figure 6. Average FM and AM sidebands, gearwheel GI, 2nd harmonic, spur runs: left sensor Sin, right sensor Sout.

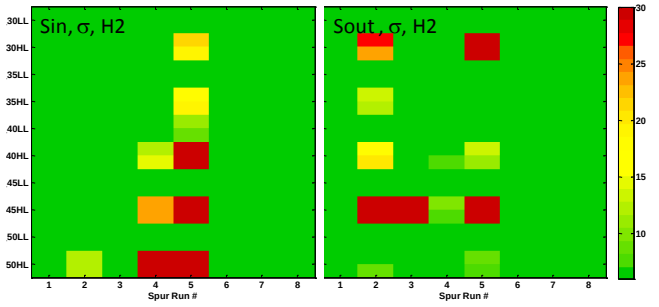

Figure 7. RMS of difference signal, 2nd harmonic, gearwheel GI, spur runs: left sensor Sin, right sensor Sout.

As can be observed in Figure 7, the RMS of the difference signal was elevated in runs 2 and 5 at high load runs but it was not consistent over the different rotating speeds.

The spectral kurtosis (Figure 8) provided a good discrimination ability (the color scale is 6-80σ, different from the 6-30 in all the other graphs). It was elevated

mainly for runs 2, 5, and 6 but it had high levels in all the runs with gear faults.

The cross-gear interference (figure not displayed) was accentuated in the first harmonic of both the RMS of the difference signal and in the average FM and AM sidebands, especially in runs 4 and 5.

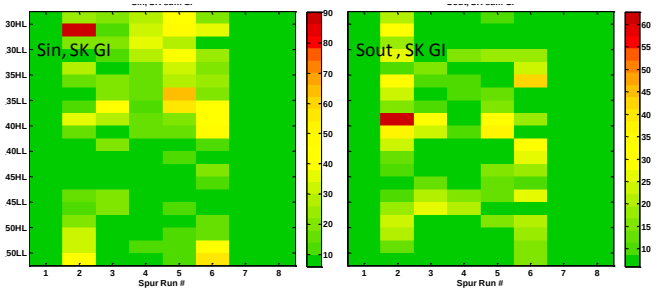

Figure 8. Sum of SK distances, gearwheel GI, spur runs: left sensor Sin, right sensor Sout.

In the spectral kurtosis results, the effect of the cross-gear interference was very clear in all the runs with a faulty gear. Apparently, the spectral kurtosis is a reliable indicator of the presence of a fault without the power to identify its exact source.

In the special case of the PHM apparatus, for the gearwheel on the input shaft, strong cross-gear interference is expected. This is because the sidebands of faulty gearwheels on the idler or output shaft always coincide with the sidebands corresponding to the input shaft.

5.2.2. Idler gear results

In the spur configuration, the 48 teeth gearwheel on the idler shaft (GM2) was eccentric in runs 2-5. The results are presented in Figure 9, Figure 10, Figure 11, and Figure 12.

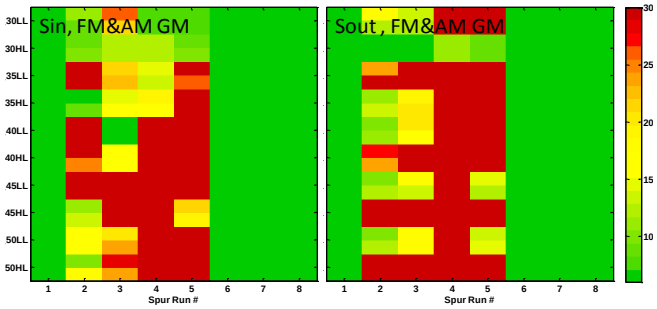

Figure 9. Average FM and AM sidebands, gearwheel GM2, 1st harmonic, spur runs: left sensor Sin, right sensor Sout.

As can be observed in Figure 10 the RMS of the difference signal is elevated in runs 2-5, mainly at high loads.

As can be observed in Figure 9, the average distance of the AM and FM peaks allows detection of the faulty runs (2-5).

Moreover, when inspecting the separate averages for FM and AM modulations (Figure 11) it can be observed that the AM average is especially high.

Similar results have been obtained for harmonics 1-3 for both the RMS of the difference and the average FM and AM sidebands.

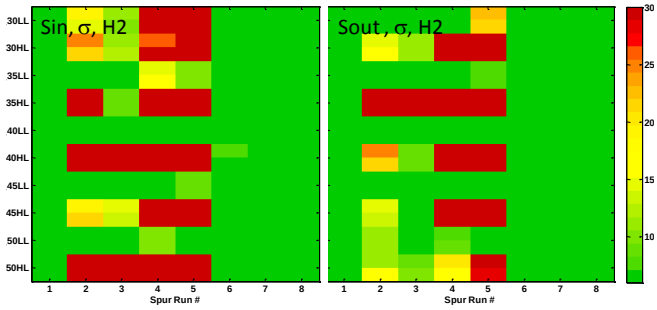

Figure 10. RMS of difference signal, 2nd harmonic, gearwheel GM2, spur runs: left sensor Sin, right sensor Sout.

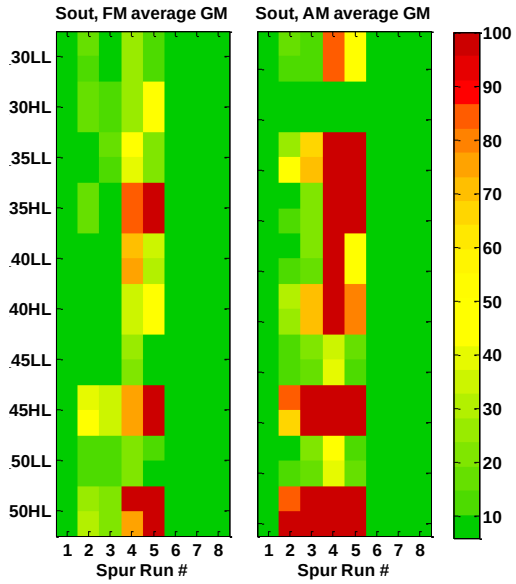

Figure 11. Average FM and AM sidebands, gearwheel GM2, harmonic 1, sensor Sout, spur runs: left average distance of FM sidebands, right average distance of AM sidebands.

Again, the spectral kurtosis (Figure 12) displayed good discrimination ability (note that the color scale is approximately 6-250σ). It is elevated mainly for runs 2-5 and with lower levels in run 6.

All the evaluated condition indicators can detect the eccentric gearwheel with a good discrimination power. The average of the FM and AM sidebands provided detailed

information about the fault nature (high amplitude modulation at few harmonics).

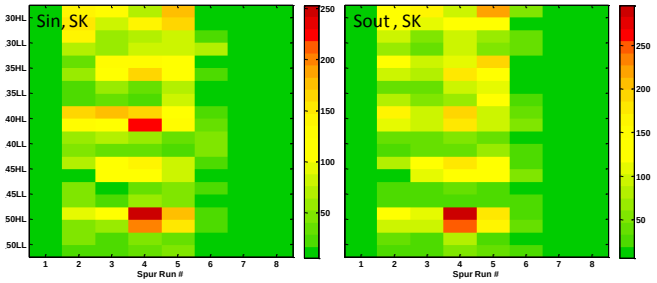

Figure 12. Sum of SK distances, gearwheel GM2, spur runs: left sensor Sin, right sensor Sout.

5.2.3. Output gear results

In the spur configuration, the gearwheel on the output shaft (GO) had a broken tooth in runs 4-6. The results are presented in Figure 13, Figure 14, and Figure 15.

As can be observed in Figure 13, the RMS of the difference signal was elevated in runs 2-5 mainly at high RPMs and high loads and only in the output sensor Sout. It meant that the findings of the RMS were not good enough to detect the broken tooth. The results were influenced by inter-component interaction and not from the faults of the output gearwheel.

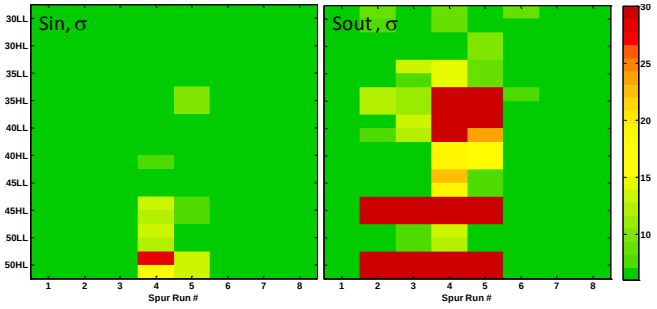

Figure 13. RMS of difference signal, 1st harmonic, gearwheel GO, spur runs: left sensor Sin, right sensor Sout.

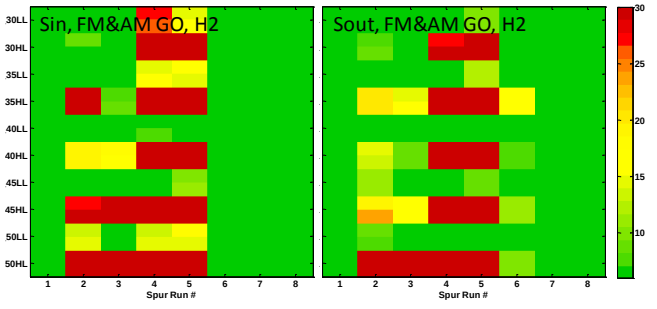

Figure 14. Average FM and AM sidebands, gearwheel GO, 2nd harmonic, spur runs: left sensor Sin, right sensor Sout.

In Figure 14, the average distance of the AM and FM sidebands allowed detection of the faulty runs 4 and 5. In sensor Sout some traces can be observed in run 6.

Run 6 had only one gear fault, the broken tooth of the output gearwheel (GO), which was not detected in the average distance of the AM and FM sidebands. Therefore, it is suspected that the high levels of the average distance of the FM and AM sidebands in runs 4 and 5 represent mainly the cross-gear interference with the eccentricity of the idler gearwheel (GM2), while the effect of the broken tooth is of low level.

The spectral kurtosis (Figure 15) provided a good discrimination capability (the color scale is approximately 6-180σ). It is elevated mainly for runs 4 and 6.

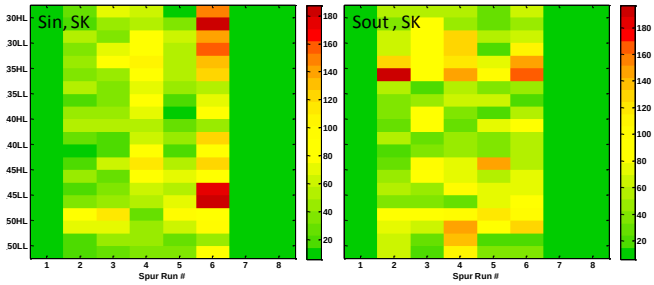

Figure 15. Sum of SK distances, gearwheel GM2, spur runs: left sensor Sin, right sensor Sout.

6. CONCLUSIONS

The evaluation of condition indicators for gear diagnostics was carried out on the PHM'09 challenge dataset in both helical and spur configurations.

Two new condition indicators for gears have been defined: the average distance of the FM and AM sidebands in the order representation of the synchronous average, and the sum of exceptional values in the distance of the spectral kurtosis based on the synchronous average.

The detection powers of the new condition indicators were compared with the even statistical moments (RMS and kurtosis) of the regular synchronous average, residual, and difference signals and their envelope.

Since all the records without gear faults have been used for the baseline generation, the comparison of features is related only to their capability of detection ignoring the potential of false alarms.

The detection powers of the statistical moments (RMS and kurtosis) were similar over the three types: regular, residual and difference.

In some cases, the RMS gave indications on the presence of faulty gears, but its detection power was found to be inferior to the other condition indicators.

The kurtosis did not discriminate between the healthy and faulty gears.

The average FM and AM sidebands displayed the best results in most of the cases, emerging as the most promising condition indicators.

The sum of exceptional spectral kurtosis values seems to allow a reliable detection of the presence of a faulty gear but without identification of the specific gearwheel or type of fault. In the helical configuration, only the spectral kurtosis was able to detect the presence of faults. However, one needs to cautious about the spectral kurtosis condition indicator. Though it showed a good potential to detect faults, we believe that this new indicator requires more research regarding the potential for false alarms. The dataset that was used in this study was not large enough to address the issue sufficiently.

The new condition indicators demonstrated the best discrimination between healthy and faulty gears in the PHM'09 dataset. Usage of these condition indicators on additional datasets with faulty gears is recommended, for further solidifying of this conclusion.

REFERENCES

Antoni J. (2006), The Spectral Kurtosis: a Useful Tool for Characterizing Non-stationary Signals, *Mechanical Systems and Signal Processing*, 20 (2004), pp282-307.

Antoni J. & Randall R. B. (2002), Differential Diagnosis of Gear and Bearing Faults, *Journal of Vibration and Acoustics*, Vol. 124, pp165-171.

Antoni J. & Randall R. B. (2004), The Spectral Kurtosis: Application to the Vibratory Surveillance and Diagnostics of Rotating Machines, *Mechanical Systems and Signal Processing*, 20 (2006), pp308-331.

Dempsey P. J. & Zakrajsek J. J. (2001), Minimizing Load Effects on NA4 Gear Vibration Diagnostic Parameter, NASA/TM—2001-210671.

Klein R., Rudyk E., Masad E. & Issacharoff M. (2011a), Emphasizing Bearing Tones for Prognostics, *The International Journal of Condition Monitoring*, Vol. 1, Issue 2, pp. 73-78.

Klein R., Rudyk E., Masad E. & Issacharoff M. (2011b), Model Based Approach for Identification of Gears and Bearings Failure Modes, *International Journal of Prognostics and Health Management*, ISSN 2153-2648, 2011 008.

Klein R., Rudyk E. & Masad E. (2011c), Decision and Fusion for Diagnostics of Mechanical Components, *Annual Conference of the Prognostics and Health Management Society*, 2011.

Lebold M., McClintic K., Campbell R., Byington C. & Maynard K. (2000), Review of vibration analysis methods for gearbox diagnostics and prognostics, *Proceedings of 54th Meeting of the Society for Machinery Failure Prevention Technology*, Virginia Beach, VA, May 1-4, 2000, pp. 623-634.

Mosher M., Pryor A. H. & Huff E. M. (2002), Evaluation of Standard Gear Metrics in Helicopter Flight Operation, *Proceedings of 56th Mechanical failure Prevention Technology Conference*, Virginia Beach, VA, April 15-19, 2002.

Zacksenhouse M., Braun S., Feldman M. & Sidahmed M. (2000), Toward Helicopter Gearbox Diagnostics from a Small Number of Examples, *Mechanical Systems and Signal Processing*, 14(4) pp 523-543.

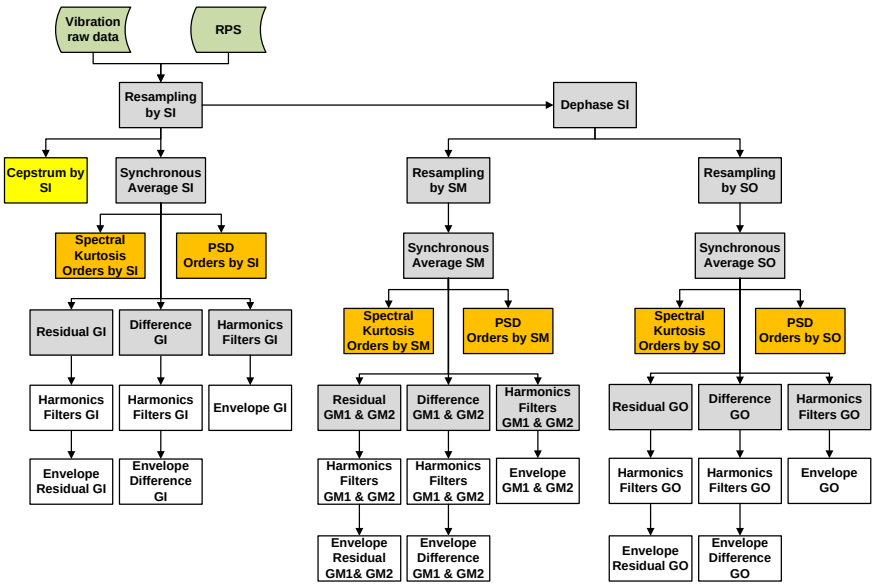

Figure 16. Flow chart of Signal Processing stage for gears of PHM'09 challenge data